Supporting Information

Impurities and Electronic Property Variations of Natural MoS_2 Crystal Surfaces

Rafik Addou[1,], Stephen McDonnell[1], Diego Barrera[1,2], Zaibing Guo[3], Angelica Azcatl[1], Jian Wang[1], Hui Zhu[1], Christopher L. Hinkle,[1] Manuel Quevedo-Lopez[1], Husam N Alshareef[4], Luigi Colombo[5], Julia W. P. Hsu[1], and Robert M. Wallace[1,*]*

[1]*Department of Materials Science and Engineering, The University of Texas at Dallas, 800 Campbell Road, Richardson Texas, 75080, Unites States*

[2]*Centro de Investigación en Materiales Avanzados, S.C. (CIMAV), Unidad Monterrey, Alianza Norte 202, 66600 Apodaca, Nuevo León, México.*

[3]*Core Labs, King Abdullah University of Science and Technology (KAUST), Thuwal 23955-6900, Saudi Arabia.*

[4]*Materials Science and Engineering, King Abdullah University of Science and Technology (KAUST), Thuwal 23955-6900, Saudi Arabia.*

[5]*Texas Instruments Incorporated, 13121 TI Boulevard, MS-365, Dallas Texas 75243, Unites States*

Contact: [*]addou@utdallas.edu, rmwallace@utdallas.edu

Highlights:

1. Impurities Detection

1.1 Inductively-coupled plasma mass spectrometry (ICPMS)

As recently noted,[1] impurities below the detection limit of XPS might impact the electronic structure of MoS_2. STM images indicate that the presence of donor and acceptor atoms in the vicinity of the topmost surface layer affects the surface topography (i.e., the electron distribution). Several impurities are detected in significant abundance using ICPMS: Al, Ca, Cu, Fe, Mg, Mn, P, Na, Ti, W, and Zn.[1] Table S1 and Table S2 show the impurities detected on another geological and synthetic chemical vapor transport (CVT) grown MoS_2 (s-MoS_2). We show also in the tables the normalized data for a Si host matrix, as such analysis is standard for the integrated circuit industry.[2] We highlight in three different colors three different levels of concentrations. The equivalent impurity concentration levels shows that this can easily exceed $5\times10^{10}/cm^2$, which is a typical *maximum* impurity concentration

Table S1. Impurity concentrations from ICPMS analysis of another geological MoS_2 sample and equivalent concentration normalized for a Si host matrix. The abundance unit is parts-per-billion by weight (pbbw). Elements highlighted by yellow are exceeding $5\times10^{10}/cm^2$, orange $>1\times10^{11}/cm^2$, and red $>1\times10^{12}/cm^2$. The gray-colored elements correspond to concentration below <0.1 ppbw.

1																	2
H																	He
3 <0.1 <5.4E10	4 <0.1 <6.4E10											5 < 0.1 1.6E10	6	7	8	9	10
Li	Be											B	C	N	O	F	Ne
11 0.14 3.2E10	12 <0.1 2.7E10											13 0.9 1.3E11	14	15	16	17	18
Na	Mg											Al	Si	P	S	Cl	Ar
19 0.3 7.1E10	20 0.2 6.7E10	21	22 0.3 7.8E10	23 <0.1 <4.4E10	24 <0.1 <4.5E10	25 <0.1 <4.6E10	26 1.2 2.4E11	27 <0.1 <4.9E10	28 <0.1 <4.8E10	29 <0.1 <5.1E10	30 <0.1 <5.2E10	31 <0.1 <6.1E11	32 <0.1 <5.6E10	33 <0.1 <5.7E10	34	35	36
K	Ca	Sc	Ti	V	Cr	Mn	Fe	Co	Ni	Cu	Zn	Ga	Ge	As	Se	Br	Kr
37	38 <0.1 <6.3E10	39	40 <0.1 <6.5E10	41 <0.1 <6.6E10	42	43	44	45	46	47 <0.1 <7.3E10	48 19.6 2.5E+12	49 <0.1 <7.6E10	50 <0.1 <7.7E10	51 1.0 3.6E11	52	53	54
Rb	Sr	Y	Zr	Nb	Mo	Tc	Ru	Rh	Pd	Ag	Cd	In	Sn	Sb	Te	I	Xe
55	56 0.4 2.2E11	*	72	73 <0.1 <1.0E11	74 4.2 1.3E12	75 0.2 1.6E11	76	77	78	79 <0.1 <1.1E11	80	81	82 1.2 5.7E11	51 11 2.6E12	84	85	86
Cs	Ba		Hf	Ta	W	Re	Os	Ir	Pt	Au	Hg	Tl	Pb	Bi	Po	At	Rn
87	88	**	104	105	106	107	108	109	110	111	112	113	114	115	116	117	118
Fr	Ra		Rf	Db	Sg	Bh	Hs	Mt	Ds	Rg	Cn	Uut	Fl	Uup	Lv	Uus	Uuo

*Lanthanide Series	57	58	59	60	61	62	63	64	65	66	67	68	69	70	71
	La	Ce	Pr	Nd	Pm	Sm	Eu	Gd	Tb	Dy	Ho	Er	Tm	Yb	Lu
**Actinide Series	89	90	91	92	93	94	95	96	97	98	99	100	101	102	103
	Ac	Th	Pa	U	Np	Pu	Am	Cm	Bk	Cf	Es	Fm	Md	No	Lr

at. #	>5E10/cm2	>1E11/cm2	>1E12/cm2	not measured
ppbw at./cm²				
Element				

specification by the Si-industry.[3]

Table S2. Impurity concentrations from ICPMS analysis of synthetic (by chemical vapor transport) MoS_2 and equivalent concentration normalized for a Si host matrix. The abundance unit is parts-per-billion by weight. Elements highlighted by yellow are exceeding $5\times10^{10}/cm^2$, orange $>1\times10^{11}/cm^2$, and red $>1\times10^{12}/cm^2$. The gray-colored elements correspond to concentration below <0.1 ppbw.

1																	2
H																	He
3 0.1 5.4E10	4 <0.1 <6.4E10											5 <0.1 <1.6E10	6	7	8	9	10
Li	Be											B	C	N	O	F	Ne
11 0.5 5.5E10	12 0.3 5.0E10											13 2.1 2.2E11	14	15	16	17	18
Na	Mg											Al	Si	P	S	Cl	Ar
19 0.5 1.0E11	20 1.0 1.8E11	21	22 0.5 1.3E11	23 <0.1 <4.4E10	24 <0.1 <4.5E10	25 <0.1 <4.6E10	26 7.4 8.3E11	27 <0.1 <4.9E10	28 <0.1 <4.8E10	29 0.5 1.4E11	30 0.1 5.5E10	31 0.1 6.1E11	32 0.1 5.6E10	33 6.1 8.8E11	34	35	36
K	Ca	Sc	Ti	V	Cr	Mn	Fe	Co	Ni	Cu	Zn	Ga	Ge	As	Se	Br	Kr
37	38 <0.1 <6.3E10	39	40 <0.1 <6.5E10	41 <0.1 <6.6E10	42	43	44	45	46	47 0.3 1.5E11	48 43.5 4.3E12	49 <0.1 <7.6E10	50 <0.1 <7.7E10	51 8.2 1.5E12	52	53	54
Rb	Sr	Y	Zr	Nb	Mo	Tc	Ru	Rh	Pd	Ag	Cd	In	Sn	Sb	Te	I	Xe
55	56 1.3 4.7E11	*	72	73 <0.1 <1.0E11	74 98.2 1.0E13	75 <0.1 <1.0E11	76	77	78	79 <0.1 <1.1E11	80	81	82 15.2 3.2E12	51 451.1 3.1E13	84	85	86
Cs	Ba		Hf	Ta	W	Re	Os	Ir	Pt	Au	Hg	Tl	Pb	Bi	Po	At	Rn
87	88	**	104	105	106	107	108	109	110	111	112	113	114	115	116	117	118
Fr	Ra		Rf	Db	Sg	Bh	Hs	Mt	Ds	Rg	Cn	Uut	Fl	Uup	Lv	Uus	Uuo
*Lanthanide Series			57	58	59	60	61	62	63	64	65	66	67	68	69	70	71
			La	Ce	Pr	Nd	Pm	Sm	Eu	Gd	Tb	Dy	Ho	Er	Tm	Yb	Lu
**Actinide Series			89	90	91	92	93	94	95	96	97	98	99	100	101	102	103
			Ac	Th	Pa	U	Np	Pu	Am	Cm	Bk	Cf	Es	Fm	Md	No	Lr

at. #				
ppbw at./cm²	>5E10/cm2	>1E11/cm2	>1E12/cm2	not measured
Element				

1.2 Time-of-Flight Secondary Ion Mass Spectrometry (ToF-SIMS)

ToF-SIMS is a surface microanalysis of both organic and inorganic materials. Secondary ions collected by bombarding process yields information about the molecular and elemental species present on the surface. This method has excellent detection limits (ppm) for most elements, which is higher than ICPMS but lower than XPS, however ToF-SIMS is broadly speaking a non-quantitative technique that can be made quantitative with suitable standards. In this work, relative sensitivity factors (RSF) for MoS_2 surface are not available in order to quantify the raw intensities of the secondary ions yields. For example, Na intensity is high but secondary ion yield is very high too. Table S3 shows the raw intensities detected in addition to the excepted

S and Mo elements. It is nevertheless seen that significant impurity concentrations can be detected.

Table S3. Raw intensities of impurities detected using ToF-SIMS method.

Raw Secondary Ion Counts in geological MoS_2						
Element	Li	B	C	O	Na	Mg
Counts	3478	22	1358	1419	2012859	4126
Element	Al	Si	S	K	Ca	V
Counts	4771	794	117356	967400	508804	8
Element	Cr	Mn	Fe	Ni	Cu	Mo
Counts	69	79	1948	31	240	2514033

1.3 X-Ray photoelectron spectroscopy (XPS) measurements.

The XPS analysis, with an elemental-specific detection limit (>0.05 at. %, ~≥5×10^{12} atoms/cm^2) that is higher than ICPMS and ToF-SIMS, was used to search for the elements indicated in Table S1. Figure S1 shows that only C and O were detected, and those contaminants can be desorbed after annealing in UHV (not shown). The arrows on the spectra in Figure S1 indicate the expected binding energy position of the contaminants.

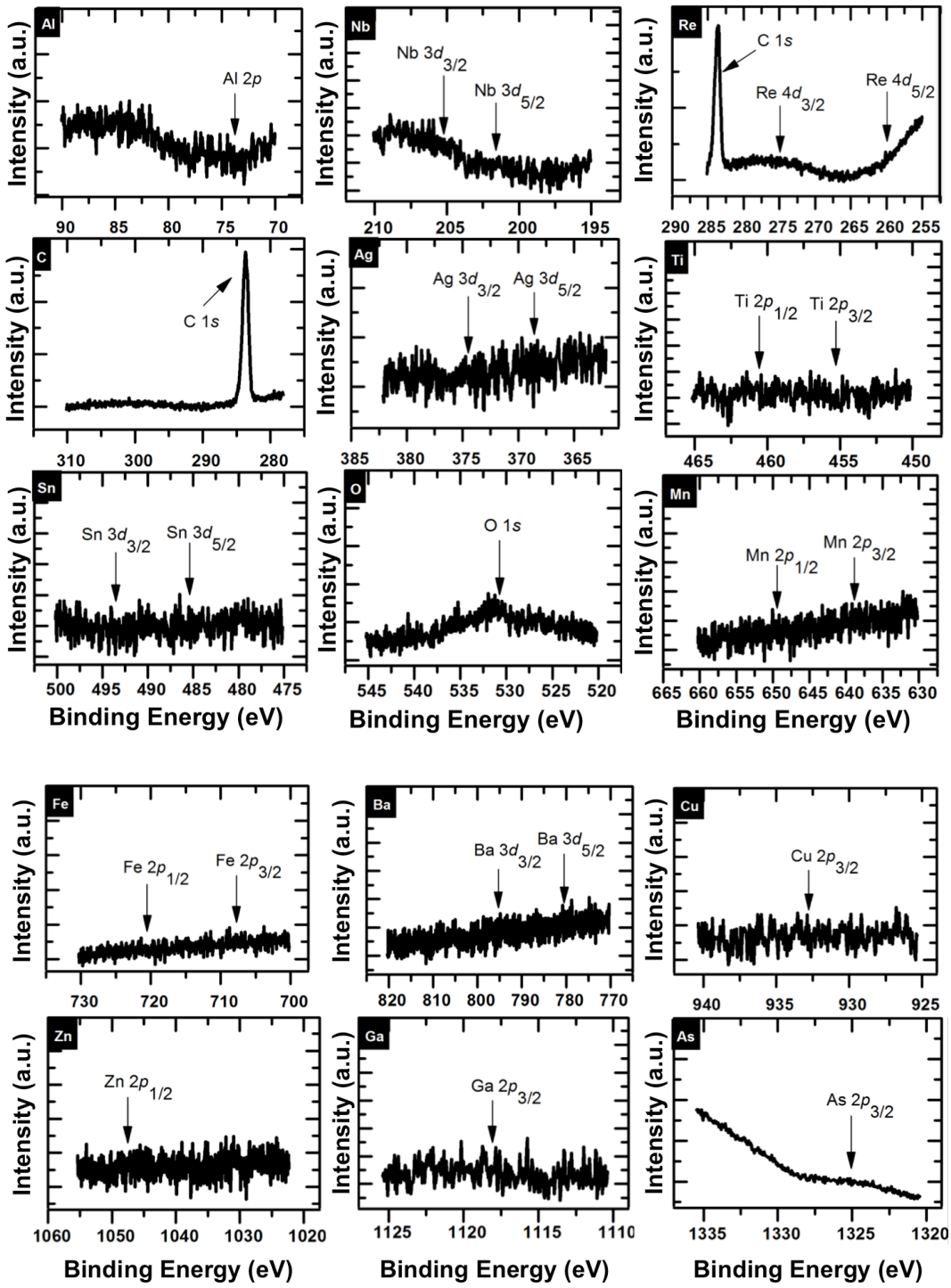

Figure S1. XPS core level measurements performed to search for impurities detected by ICPMS and ToF-SIMS. All impurities are below the detection limit.

2. Work Function Variation

In addition to the work function (WF) shown in the main text carried out on three different samples, the WF was measured on three other natural MoS_2 samples immediately after exfoliation under the same ambient conditions. Table S4 shows the experimental values obtained by Kelvin probe. On separate sample (#4), the WF was measured on five different locations before (Figure S2(a)) and after exfoliation (Figure S2(b)) as indicated in Table S5.

Table S4. Workfunction measurements measured on three different samples immediately after exfoliation.

	Sample 1	**Sample 2**	**Sample 3**
WF after exfoliation (eV)	5.15 ± 0.20	4.45± 0.20	5.1± 0.20

Table S5. The work function measurements of five different spots on the same sample measured immediately after exfoliation.

Location	WF before exfoliation (eV)	WF after exfoliation (eV)
1	4.79	5.23
2	5.07	4.94
3	4.75	5.03
4	4.87	5.33
5	4.85	5.32
Average	**4.87± 0.12**	**5.17± 0.18**

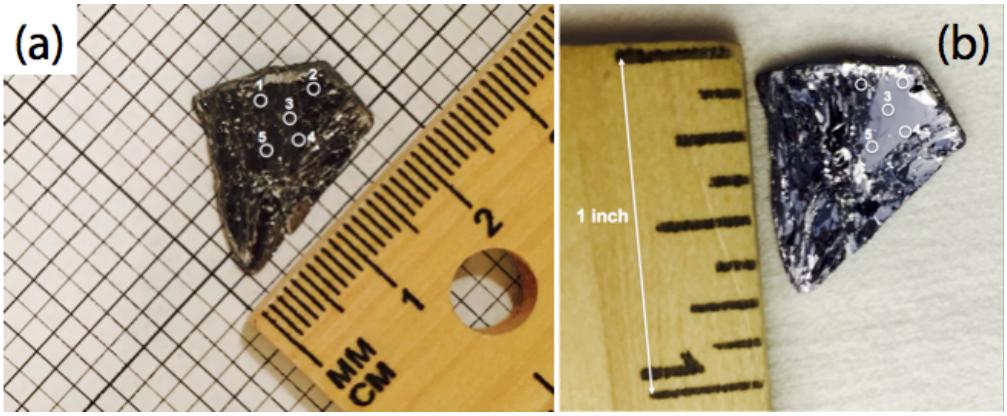

Figure S2. Large MoS_2 sample before (a) and after (b) exfoliation.

3. Surface characterization of synthetic MoS_2.

We compared the surface characteristics of geological sample (g-MoS_2) to the synthetic CVT grown sample (Figure S3a). We characterized the surface of the s-MoS_2 using room temperature scanning tunneling microscopy and spectroscopy (STM and STS). The low magnification STM image in Figure S3b shows a high density of dark defects, comparable to previous reports on geological samples[1] and to that shown in Figure 7. The dark defects are more noticeable in the higher magnification STM image in Figure S3c. An example of the dimensions of the dark defect is presented in Figure S3d. A single dark defect is characterized by a width of ~2-3 nm and depth of ~0.4 nm. Such defects can be explained in part by the presence of impurities at or underneath the topmost surface layer. Structural defects such as voids are also observed. The surface topography obtained by STM suggests the presence of the same imperfections on both synthetic and geological MoS_2 and the defect density change even across the same surface.

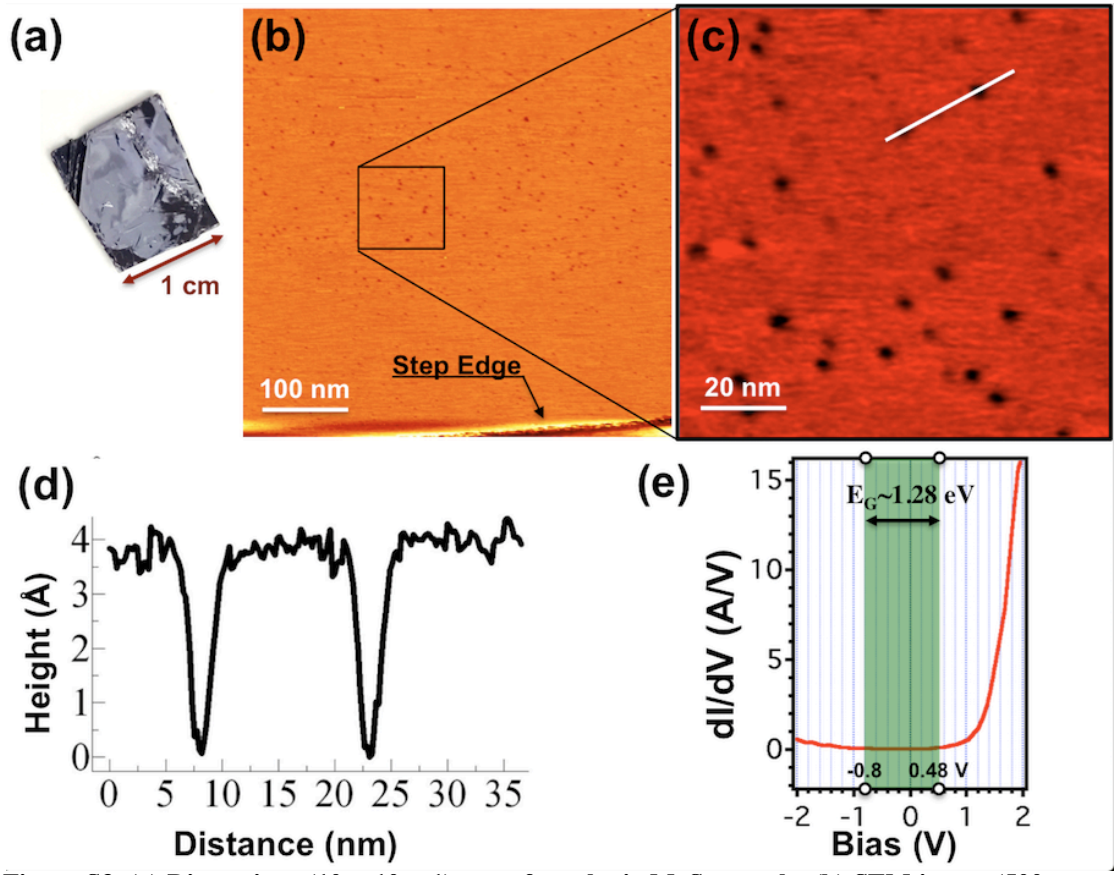

Figure S3. (a) Dimensions (10 × 10 × 1) *mm* of synthetic MoS_2 sample. (b) STM image (500 *nm* × 500 *nm*) showing high defect density. (c) STM image (100 *nm* × 100 *nm*). The line profile across the white line is presented in panel (d). (e) STS curve recorded on s-MoS_2 surface.

Analyzing the STS spectra measured on s-MoS_2 surface shows a band gap of about 1.28 eV (Figure S3e) in agreement with previously reported band bap[1]. As indicated in Figure S3e, the Femi level is not located at the conduction band minimum (CBM). We located the valence band maximum (VBM) at -0.8 V and the CBM at 0.48 V. This shift is expected due to the presence of imperfections causing spatial variations of the Fermi level position on MoS_2 bulk crystal surfaces.[1,4]

The synthetic crystal, "s-MoS_2" was also characterized using Kelvin probe and photoelectrons spectroscopy in air (PESA). The WF measured immediately after exfoliation is about 5.18±0.01 eV. As for geological MoS_2, the WF decreases with time and stabilizes after ~20 min to reach ~5.12±0.01 eV (Figure S3). The ionization potential (i.e. the valence band maximum) is measured at 5.72±0.05 eV. Using

reported and measured bandgap (E_g ~1.3 eV), the electron affinity is estimated at ~4.4 eV. Our measurements (VBM, WF, and E_G) indicate that the s-MoS_2 crystal is p-type.

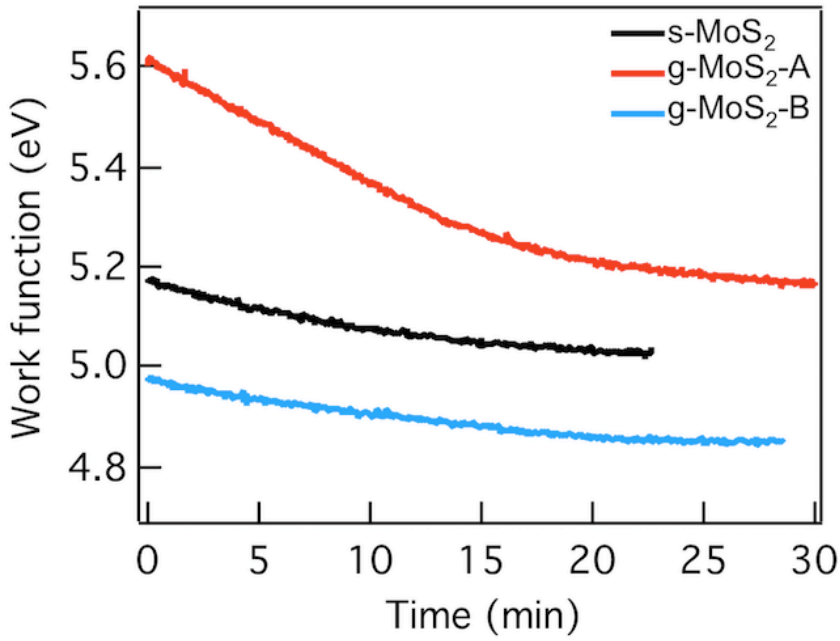

Figure S4. Kelvin probe measurements of the work function of synthetic s-MoS_2 in comparison to geological crystals (g-MoS_2).

References and Notes.

1. Addou, R.; Colombo, L.; Wallace, R. M. Surface Defects on Natural MoS_2. *ACS Appl. Mater. Interfaces* **2015**, 7, 11921-11929.

2. For example, see: Beebe, M. and Anderson, S. Monitoring wafer cleanliness and metal contamination via VPD ICP-MS: Case studies for next generation requirements. *Microelectron. Eng.* **2010**, 87, 1701-1705.

3. See the latest industry roadmap document for specifications: www.itrs.net.

4. McDonnell, S.; Addou, R.; Buie, C.; Wallace, R. M.; Hinkle, C. L. Defect-Dominated Doping and Contact Resistance in MoS_2. *ACS Nano* **2014**, 8, 2880-2888.